1,3-Bis(2-thienylmethylene)-1*H*,3*H*-thieno[3,4-*c*]thiophene: A Precursor for a New Low Band Gap Polymer

Michael Hanack[a]*, Ulrich Schmid[a], Ursula Röhrig[a], Jean-Marc Toussaint[b], Christine Adant[b], and Jean-Luc Brédas[b]

Institut für Organische Chemie, Lehrstuhl für Organische Chemie II[a],
Universität Tübingen, Auf der Morgenstelle 18, D-W-7400 Tübingen, Germany

Service de Chimie des Matériaux Nouveaux[b],
Université de Mons-Hainaut, Place du Parc 20, B-7000 Mons, Belgium

Received December 4, 1992

Key Words: Polymers, low band gap / Polyarenemethylenes / 1*H*,3*H*-Thieno[3,4-*c*]thiophene derivative

A new precursor, 1,3-bis(2-thienylmethylene)-1*H*,3*H*-thieno-[3,4-c]thiophene (**9**), for polyarenemethylenes (PAM), which are predicted to be low band gap polymers, is obtained by a Knoevenagel-type condensation of 1*H*,3*H*-thieno[3,4-c]thiophene 2-oxide (**7**) with 2-thiophenecarbaldehyde followed by reduction of the intermediate sulfoxide **8** with 2-chloro-1,3,2-benzodioxaphosphole. Several investigations with cyclic voltammetry and UV-Vis-NIR spectroelectrochemistry (SEC) are carried out on **9**. The experimental data are compared with the results of electronic band structure calculated on the basis of an MNDO-optimized geometric structure by VEH pseudopotential method.

Polymeric materials which exhibit conducting properties like polyacetylene (PA)[1], poly-*p*-phenylene (PPP)[2], polypyrrole (PPy)[3], and polythiophene (PT)[4] have been extensively studied. These polymers, however, gain a high conductivity only after chemical or electrochemical oxidative (p) or reductive (n) doping. The thermal and chemical stability of the doped polymers is often not very high. Non-doped systems with a low band gap which at least show semiconducting properties are interesting targets for syntheses.

Based on VEH (Valence Effective Hamiltonian) calculations, it has been shown that in polymers related to PPy and PT the band gap E_g is a function of the quinoid character of these polymers[5]. As a result of decreasing bond-length alternation along the C–C backbone, the band gap becomes smaller. Thus, with increasing quinoid character of the subunits the band gap E_g decreases. A low band gap besides intrinsic conductivity may lead to interesting non-linear optical properties of the polymer.

The first example of a low band gap polymer is polyisothianapthene (PITN) with a band gap of $E_g \approx 1$ eV[6], which corresponds to half the band gap value of PT. The ring annulation in PITN stabilizes the quinoid contributions in the ground state in comparison with PT.

VEH[7] and extended Hückel[8] calculations have shown polymers of the general formula given in Figure 1 also to possess a small band gap ($\approx$ 1 eV). These methine-bridged molecules are known as polyarenemethylenes (PAM); because of the low band gap, they are predicted to have intrinsic semiconducting properties[9].

Several precursor molecules for polyarenemethylenes have been synthesized by our group, e.g. 1,3-dihydro-1,3-bis(2-thienylmethylene)isothianapthene (**1**, X = Y = S, Z = HC=CH) which is obtained by a Knoevenagel-type condensation of 1,3-dihydroisothianapthene 2-oxide with 2-thiophenecarbaldehyde and reduction of the corresponding sulfoxide with 2-chloro-1,3,2-benzodioxaphosphole[9b,11].

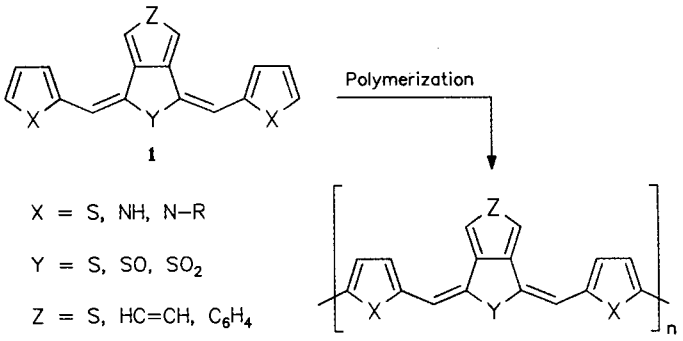

Figure 1. General formula of the precursors **1** and the polyarenemethylenes

Electrochemical oligomerization of 1,3-dihydro-1,3-bis(2-thienylmethylene)isothianaphthene (**1**, X = Y = S, Z = HC=CH) on a platinum electrode affords the corresponding oligomer (Figure 1) as a black layer. The cyclic voltammogram of **1** (X = Y = S, Z = HC=CH) shows the typical shape for electrochemical oligomerization, the electrochemically formed layer is electroactive. It is possible to oxidize and reduce the film in several cycles. A spectroelectrochemical measurement of the oligomerization process shows a red shift of about 130 nm of the resulting oligomer in comparison with the monomer **1**[9]. Other precursor molecules **1** with X = S, N–H, N–R, Y = S, SO, SO_2, and Z = S, HC=CH have also been synthesized by us and their electrochemical oligomerization has been studied[9]. The band gaps of the corresponding oligomers have been determined to be 1.5–1.7 eV[9e]. For other attempts to obtain polyrenemethylenes see refs.[9b,10].

  0009–2940/93/0606–1487 $ 10.00+.25/0

Based on MO calculations (vide infra) 1,3-bis(2-thienylmethylene)-1*H*,3*H*-thieno[3,4-*c*]thiophene (**9**) is another promising precursor molecule for low band gap polymers. As shown below the band gap of the corresponding polymer **10** (Scheme 1) is calculated to be $E_g \approx 1.57$ eV. In addition to the band gap calculations for **10** we report here on the synthesis of the precursor **9** and first results on its electrochemical oligomerization.

Synthesis

The synthesis of **9** follows the route given in Scheme 1. The Knoevenagel-type condensation of the sulfoxide **7** with 2-thiophenecarbaldehyde is carried out in methanol. The methylene groups in **7**, activated by the sulfoxide group, react smootly with 2-thiophenecarbaldehyde to give the corresponding air-stable methine-bridged sulfoxide **8** in satisfactory yield. The sulfoxide group in **8** is reduced with 2-chloro-1,3,2-benzodioxaphosphole[9b,11] in toluene to yield **9**. Several methods for the synthesis of **6** have been reported[12]. We have used a new route for the synthesis of **6** according to Scheme 1 combining known reactions described in the literature (see Experimental).

Scheme 1

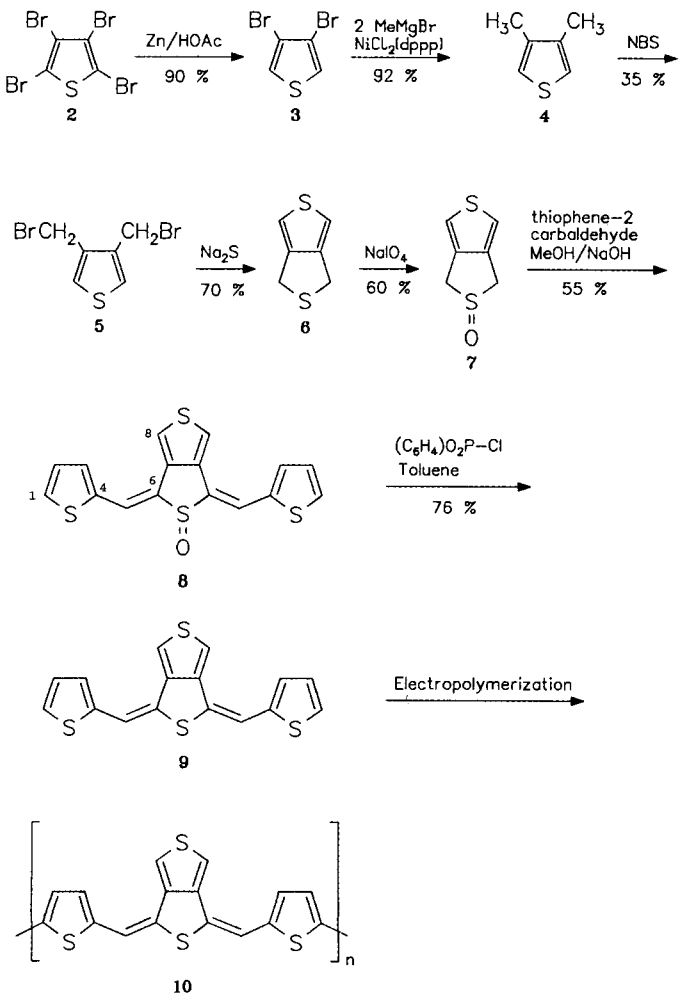

Cyclic Voltammetric Studies

The electrochemical oxidation of **9** is carried out in a cell containing dichloromethane as the solvent and tetrabutylammonium hexafluorophosphate as supporting electrolyte with platinum as a working electrode.

Figure 2 shows the cyclic voltammogram of the electrooligomerization of **9** (multisweep, 8 cycles, 0.2 to 1.8 V). In the first cycle the oxidation of the monomer occurs at 0.95 V vs. SCE. The second and following cycles show an additional oxidation at a lower potential. This signal is assigned to the oxidation of the formed oligomer. With increasing number of cycles the current increases due to the formation of an electroactive black oligomer layer on the working electrode surface. The oligomerization proceeds much better at higher potentials (Figure 2b). The peak currents caused by oligomerization soon after the formation of the monocation are very small (Figure 2a). Increasing of the anodic switching potential leads to higher peak currents of the formed oligomers. The formed layers show a reversible charging and discharging behaviour. This electroactivity can be seen in CV and SEC investigations of the formed layers in a blank monomer-free solution.

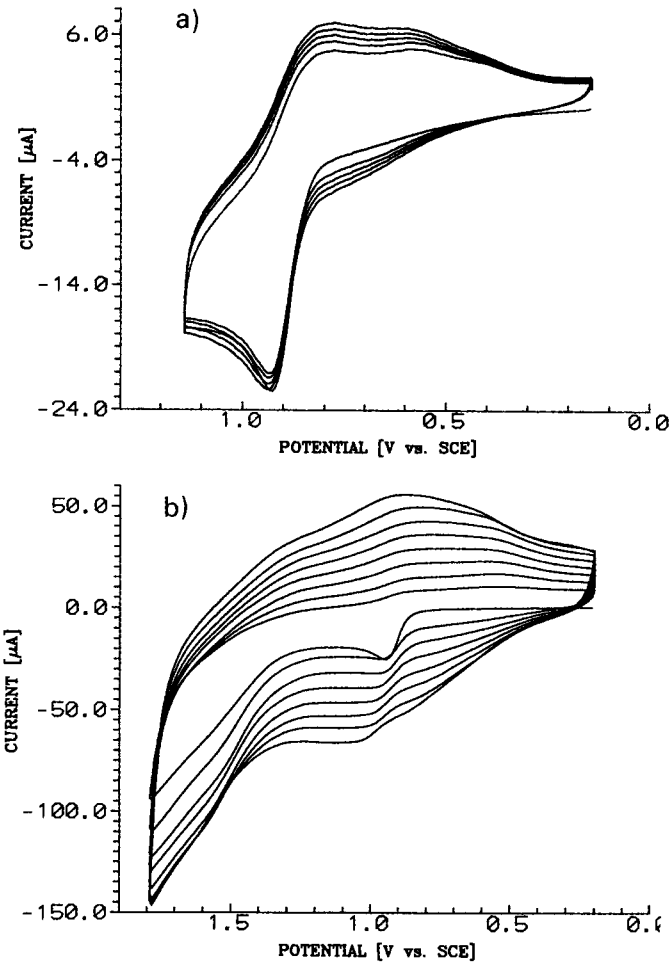

Figure 2. Multisweep voltammogram of 1,3-bis(2-thienylmethylene)-1*H*,3*H*-thieno[3,4-*c*] thiophene (**9**) with an anodic switching potential of a) 1.15 V vs SCE (5 cycles) and b) 1.78 V vs SCE (8 cycles) (scan rate 100 mV/s, solvent 1,2-dichloroethane/*n*-Bu_4NPF_6)

UV-Vis-NIR-spectroelectrochemical investigations of the oligomerization of **9** on ITO-(Indium Tin Oxide-)coated Pyrex glass show the disappearance of specific absorptions at 324, 345, 382, and 405 nm with increasing potential. Simultaneously, new absorptions of the oxidatively formed products at 660 and 850 nm (very broad) are observed due to the formation of oligomers. Because of the enlarged conjugated π-electron system in the oligomer compared to the monomer the absorptions are red-shifted. From the UV absorption of the completely reduced oligomer layer on ITO in a blank monomer-free solution we obtain a band gap value of about 1.8 eV (Figure 3). Only at high cathodic potentials the layer is completely reduced, leading to a dissapearance of the UV-Vis-NIR absorptions assigned to the oxidized form of the oligomer. A comparison of the experimental band gap value of the completely reduced layer with the VEH-based theoretical data on the oligomers given in Table 1 indicates that an oligomer with short chain length is formed. The formation of only dimers is unlikely, because unsoluble stable layers are formed. The dimer of the related compound 1,3-dihydro-1,3-bis(2-thienylmethylene)isothianaphthene (Figure 1; X = Y = S, Y = S, Z = HC=CH) has been isolated and identified by FD-MS and forms a red solution in dichloromethane[9e].

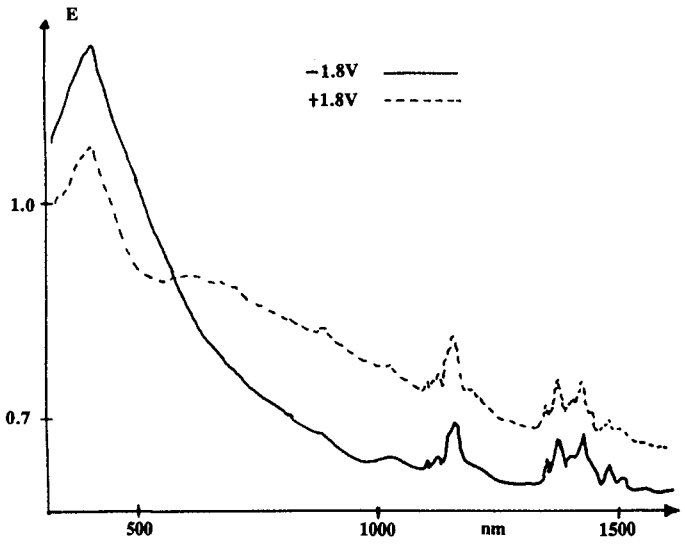

Figure 3. Spectrochemical investigation of an oligomer layer of 1,3-bis(2-thienylmethylene)-1*H*,3*H*-thieno[3,4-*c*]thiophene (**9**) (solvent CH_2Cl_2/*n*-Bu_4NPF_6; working electrode: electrochemically coated ITO glass)

Table 1. VEH-calculated electronic parameters for the oligomers of 1,3-bis(2-thienylmethylene)-1*H*,3*H*-thieno[3,4-*c*]thiophene (**9**) in the solid state (values in eV)

	Monomer	Dimer	Trimer
Ionization potential	5.06	4.77	4.69
Electron affinity	−2.90	−2.96	−3.04
π-π* transition	2.47	1.81	1.65

The sulfoxide **8** can also be electrochemically oligomerized, but the value of the oxidation potential lies near the solvent limit. The formed layer shows also electroactivity. A more detailed account of the electrochemical studies on thiophene-based low band gap polymers will be reported in ref.[9e].

Band Gap Calculations of 1,3-Bis(2-thienylmethylene)-1*H*,3*H*-thieno[3,4-*c*]thiophene Systems

Methodology: The methodology of calculations is identical to that previously used successfully[13]. The geometrical optimization of poly-1,3-bis(2-thienylmethylene)-1*H*,3*H*-thieno[3,4-*c*]thiophene (PTMTT) (**10**) is carried out by means of the MNDO method[14] as implemented in the MOPAC 6.0 software[15]. This semiempirical technique is known to afford good geometrical estimates in organic molecules. In a second step, the central part of the optimized oligomer is used as input for the band structure calculations by means of the VEH pseudopotential method[16]. VEH has been shown to provide accurate determinations of essential electronic parameters in organic molecules and polymers, such as ionization potential, electron affinity, band gap energy, or highest occupied band width[17].

Geometry Optimization Results: In the course of the MNDO geometry optimization, PTMTT (**10**) is forced to remain planar. Due to the presence of an odd number of conjugated carbons between the thiophene and thieno[3,4-*c*]thiophene units, these units alternate between aromatic and quinoid geometries. The geometries for the thiophene and thieno[3,4-*c*]thiophene rings in **10** are identical to those optimized within the MNDO method for the homopolymers, i.e. for polythiophene (PT) (**11**) in its ground state and for a polythieno[3,4-*c*]thiophene (PTT) (**12**) chain adopting a quinoid geometry.

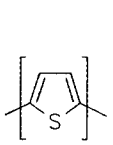

11

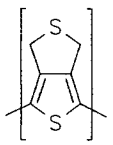

12

The valence bond angle of the conjugated carbon between thiophene and the quinoid moiety is 135° which minimizes the steric hindrance between hydrogen atoms on the thiophene and thieno[3,4-*c*]thiophene units.

Electronic Structure Results: The VEH-calculated band gap for PTMTT is of 1.57 eV, i.e. 0.22 eV smaller than the one calculated for polythiophene in its ground state on the basis of an MNDO-optimized geometric structure. The band structure of PTMTT is depicted in Figure 4.

In order to interpret the calculated band gap in PTMTT (**10**), we proceed as described in ref.[19], the bonding-antibonding electronic patterns (i.e. the signs of the LCAO coefficients) appearing on top of the valence (HOMO) band and at the bottom of the conduction (LUMO) band of **10** are analyzed and compared with those of "aromatic" PT and "quinoid" PTT. The electronic characters of the HOMO and LUMO levels of PTMTT are given in Figure 5. The electronic characteristics given for "aromatic" polythio-

phene and "quinoid" polythienothiophene are those determined for these two chains when the systems adopt the geometry of the thiophene and thienothiophene units in PTMTT, respectively.

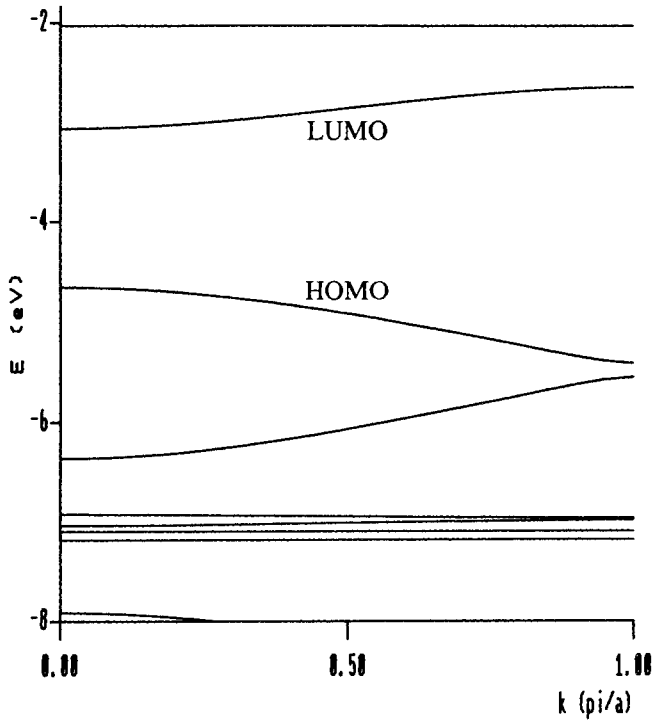

Figure 4. VEH band structure of PTMTT (**10**). Only the highest occupied and the lowest unoccupied bands are represented

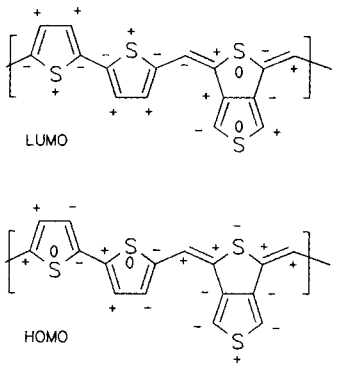

Figure 5. Bonding-antibonding electronic patterns of the HOMO (top) and LUMO (bottom) levels of PTMTT (**10**)

The analysis of the LCAO coefficients in PTMTT (**10**) indicates that:

(i) On the HOMO, the thiophene rings (with an aromatic geometry) possess aromatic electronic characters and the thieno[3,4-*c*]thiophene ring possesses quinoid electronic characters (by aromatic or quinoid electronic character, we mean that the bonding-antibonding pattern of the LCAO coefficients are consistent with an aromatic or quinoid geometry).

(ii) On the LUMO, there is an inversion of the electronic characters relative to the HOMO, so that the thiophene units show quinoid electronic patterns and the thieno[3,4-*c*]thiophene unit presents aromatic electronic characters. Compared to the bonding-antibonding electronic patterns appearing on the HOMO and LUMO levels of "aromatic" PT and "quinoid" PTT, it appears that the HOMO of PTMTT is a mixing of the HOMO's of "aromatic" PT and "quinoid" PTT while the LUMO of PTMTT is a mixing of the LUMO's of "aromatic" PT and "quinoid" PTT.

As a result, the HOMO and the LUMO bands of PTMTT lie between the corresponding levels of the constituting units:

– the HOMO level of PTMTT (–4.66 eV) lies between the HOMO of "aromatic" PT (–4.84 eV) and the HOMO of "quinoid" PTT (–4.46 eV);

– the LUMO of PTMTT (–3.09 eV) is located between the LUMO of "aromatic" PT (–3.05 eV) and the LUMO of "quinoid" PTT (–2.87 eV) (see Table 2).

Table 2. MNDO-based VEH values (in eV) for highest occupied band width (HOBW), ionization potential (IP), electron affinity (EA), and band gap energy (E_g) of PTMTT (**10**), "aromatic" polythiophene ("arom." PT) and "quinoid" polythienothiophene ("quin." PTT). The electronic structures given for "aromatic" polythiophene and "quinoid" polythienothiophene are the ones determined when the systems adopts the geometry of the thiophene and thienothiophene units in PTMTT, respectively

	HOBW	IP	EA	E_g
PTMTT	0.74	4.66	–3.09	1.57
"arom." PT	2.07	4.84	–3.05	1.79
"quin." PTT	1.97	4.46	–2.87	1.59

This work was supported by *Bundesministerium für Forschung und Technologie*. The authors also thank the *Wacker-Chemie GmbH* for financial support. This work was also partly supported by *Programme Gouvernemental Belge d'Impulsion en Technologie de l'Information* (contract IT-SC-22) and by the *Pôle d'Attraction Interuniversitaire Belge: Chimie Supramoléculaire et Catalyse*.

Experimental

Melting points: uncorrected. – ^{1}H and ^{13}C NMR: Bruker AC 250 (^{1}H, 250 MHz; ^{13}C, 62.5 MHz). – FTIR: Bruker IFS 48. – MS: Varian MAT 711 (70 eV). – Elemental analyses: Carlo Erba Analyser 1104, 1106.

Thiophene, 2-thiophenecarbaldehyde, [$NiCl_2$(dppp)] [dppp = 1,3-bis(diphenylphosphanyl)propane] and 2-chloro-1,3,2-benzodioxaphosphole are commercially available. Tetrabromothiophene (**2**)[18], 3,4-dibromothiophene (**3**)[19], 3,4-dimethylthiophene (**4**)[20], 3,4-bis(bromomethyl)thiophene (**5**)[17], 1*H*,3*H*-thieno[3,4-*c*]-thiophene (**6**)[21], and 1*H*,3*H*-thieno[3,4-*c*]thiophene 2-oxide (**7**)[22] were prepared according to literature procedures. – The pure products were isolated by flash chromatography (silica gel 40–63 μm).

1,3-Bis(2-thienylmethylene)-1H,3H-thieno[3,4-c]thiophene 2-Oxide (**8**): 0.81 g (5.1 mmol) of 1*H*,3*H*-thieno[3,4-*c*]thiophene 2-oxide (**7**) and 1.25 g (11.1 mmol) of 2-thiophenecarbaldehyde were dissolved in a solution of 0.55 g of NaOH in 35 ml of methanol. The solution was stirred at room temp. for 3 d. The reaction mixture was chromatographed on a silica gel column with ethanol, and after evaporation of the solvent the precipitate was purified with dichloromethane in a Soxhlet extractor. Evaporation of the solvent yielded 965 mg (54.5%) of a yellow powder, m.p. *222*–228 °C (dec.).

– IR (KBr): $\tilde{\nu} = 3082\ cm^{-1}$ (CH st), 3063, 1618, 1597 (ar CH), 1599, 1148 (γ-CH), 1418, 1390, 1360, 1223, 1051, 1007 (S=O), 856, 843 (γ-CH), 785 (γ-CH), 714 (C–S). – ^1H NMR ([D$_6$]DMSO): δ = 7.99 (s, 2H, 5-H), 7.86 (s, 2H, 8-H), 7.85 (d, $J_{3,2} = 3.25$ Hz, 2H, 3-H), 7.60 (d, $J_{1,2} = 3.39$ Hz, 2H, 1-H), 7.235 (dd, $J_{1,2} = 8.71$, $J_{2,3} = 1.10$ Hz, 2H, 2-H). – ^{13}C NMR ([D$_6$]DMSO): δ = 140.96 (C-6), 137.07 (C-7), 135.26 (C-4), 132.38 (C-3), 131.47 (C-2), 128.40 (C-1), 124.30 (C-8), 117.33 (C-5). – UV (CH_2Cl_2): $\lambda_{max} = 328$ nm. – MS, *m/z* (%): 346 [M^+], 330 (100) [$M^+ - O$], 296, 264 [$M^+ - S$], 249, 235, 221, 190, 148, 126, 111, 97, 69, 45. – $C_{16}H_{10}OS_4$ (346.5): calcd. C 55.46, H 2.91; found C 54.84, H 3.02.

1,3-Bis(2-thienylmethylene)-1H,3H-thieno[3,4-c]thiophene (**9**): 106.5 mg (0.61 mmol) of 2-chloro-1,3,2-benzodioxaphosphole was added under nitrogen to a solution of 204 mg of **8** in 16.8 ml of dry toluene and 0.056 ml of pyridine during 15 min. The solution was stirred at room temp. for 24 h and refluxed for 1 h. The reaction mixture was chromatographed on silica gel with ether/*n*-hexane (2:1). Evaporation of the solvent afforded 176.5 mg (76.4%) of a yellow product, m.p. 145–149 °C. – IR (KBr): $\tilde{\nu} = 3854\ cm^{-1}$, 3746, 3099 (CH st), 2926, 2854, 1653 (ar C–C), 1558, 1541, 1506, 852 (γ-CH), 766, 692 (C–S), 667. – ^1H NMR ([D$_6$]DMSO): δ = 7.90 (s, 2H, 5-H), 7.70 (d, $J_{3,2} = 4.91$ Hz, 2H, 3-H), 7.65 (s, 2H, 8-H), 7.27 (d, $J_{1,2} = 3.01$ Hz, 2H, 1-H), 7.20 (dd, $J_{2,1} = 8.69$, $J_{2,3} = 1.4$ Hz, 2H, 2-H). – ^{13}C NMR ([D$_6$]DMSO): δ = 144.23 (C-6), 140.00 (C-4), 128.07 (C-3), 127.74 (C-2), 127.38 (C-7), 127.22 (C-1), 115.35 (C-8), 111.78 (C-5). – UV (CH_2Cl_2): $\lambda_{max} = 380$ nm. – MS, *m/z* (%): 330 (100) [M^+], 296 [$M^+ - S$], 264 [$M^+ - 2\ S$], 253, 165, 149, 127, 70. – $C_{16}H_{10}S_4$ (330.5): calcd. C 58.16, H 3.05; found C 59.26, H 3.60.

[1] H. Naarmann, N. Theophilou, *Synth. Met.* **1987**, *22*, 1.
[2] [2a] L. W. Shacklette, R. R. Chance, D. M. Ivoroy, G. G. Miller, R. H. Baughman, *Synth. Met.* **1979**, *1*, 307. – [2b] S. Aeiyach, P. Soubiran, P. C. Lacaze, G. Froyer, Y. Pelous, *Synth. Met.* **1989**, *32*, 107.
[3] [3a] A. F. Diaz, K. K. Kanazawa, G. R. Gardini, *J. Chem. Soc., Chem. Commun.* **1979**, 635. – [3b] F. P. Bradner, J. S. Shapiro, *Synth. Met.* **1988**, *26*, 69.
[4] [4a] G. Tourillon, F. Garnier, *J. Electroanal. Chem.* **1982**, *135*, 173. – [4b] W. Kobel, H. Kiess, M. Egli, *Synth. Met.* **1988**, *22*, 265.
[5] J. L. Brédas, *J. Chem. Phys.* **1985**, *82*, 3808.
[6] F. Wudl, M. Kobayashi, A. J. Heeger, N. Colaneri, *J. Chem. Phys.* **1985**, *82*, 5717.
[7] J. L. Brédas, *Springer Ser. Solid State Sci.* **1985**, *63*, 166.
[8] M. Kertesz, Y.-S. Lee, *J. Chem. Phys.* **1988**, *88*, 209.
[9] [9a] M. Hanack, G. Hieber, G. Dewald, H. Ritter, *Synth. Met.* **1991**, *41–43*, 2979. – [9b] G. Hieber, M. Hanack, K. Wurst, J. Strähle, *Chem. Ber.* **1991**, *124*, 1597. – [9c] M. Hanack, G. Hieber, K.-M. Mangold, H. Ritter, U. Röhrig, *Mat. Res. Soc. Symp. Proc.* **1992**, *1247*, 637. – [9d] M. Hanack, G. Hieber, K.-M. Mangold, H. Ritter, U. Röhrig, U. Schmid, *Synth. Met.* **1993**, in print. – [9e] M. Hanack, K.-M. Mangold, U. Röhrig, *J. Am. Chem. Soc.*, in print.
[10] [10a] R. Becker, G. Blöchl, H. Bräunling, *Springer Ser. Solid State Sci.* **1989**, *91*, 465. – [10b] R. Jira, H. Bräunling, *Synth. Met.* **1987**, *17*, 691.
[11] D. W. Chasar, T. M. Pratt, *Synthesis* **1976**, 262.
[12] [12a] D. J. Zwanenburg, H. Wynberg, *J. Org. Chem.* **1964**, *29*, 1919. – [12b] D. J. Zwanenburg, H. Wynberg, *J. Org. Chem.* **1969**, *34*, 333. – [12c] J. Nakayama, A. Ishii, Y. Kobayashi, M. Hoshino, *J. Chem. Soc., Chem. Commun.* **1988**, 959.
[13] [13a] J. M. Toussaint, B. Thémans, J. M. André, J. L.Brédas, *Synth. Met.* **1989**, *28*, C205. – [13b] J. M. Toussaint, F. Wudl, J. L. Brédas, *J. Chem. Phys.* **1989**, *91*, 1783. – [13c] J. M. Toussaint, J. L. Brédas, *J. Chem. Phys.* **1991**, *94*, 8122. – [13d] J. M. Toussaint, J. L. Brédas, *Synth. Met.* **1992**, *46*, 325.
[14] M. J. S. Dewar, W. Thiel, *J. Am. Chem. Soc.* **1977**, *99*, 4899, 4907.
[15] H. A. Kurtz, J. J. P. Stewart, K. M. Dieter, *J. Comp. Chem.* **1990**, *11*, 82.
[16] J. M. André, L. A. Burke, J. Delhalle, G. Nicolas, Ph. Durand, *Int. J. Quantum Chem. Symp.* **1979**, *13*, 283.
[17] [17a] J. L. Brédas, R. R. Chance, R. Silbey, G. Nicolas, Ph. Durand, *J. Chem. Phys.* **1981**, *75*, 255. – [17b] J. L. Brédas, R. H. Baughman, R. R. Chance, R. Silbey, *J. Chem. Phys.* **1982**, *76*, 3673. – [17c] J. L. Bréderas, R. L. Elsenbaumer, R. R. Chance, R. Silbey, *J. Chem. Phys.* **1983**, *78*, 5656.
[18] W. Steinkopf, H. Jacob, H. Penz, *Liebigs Ann. Chem.* **1934**, *512*, 136.
[19] S. Gronowitz, *Acta Chem. Scand.* **1959**, *13*, 1045.
[20] M. Kumada, K. Tamao, S. Kodama, I. Nakajima, *Tetrahedron* **1982**, *38*, 3347.
[21] M. P. Cava, R. L. Shirley, *J. Am. Chem. Soc.* **1960**, *82*, 654.
[22] M. P. Cava, N. M. Pollac, O. A. Mamer, M. J. Mitchell, *J. Org. Chem.* **1971**, *36*, 3933.

[439/92]